JOURNAL OF TISSUE ENGINEERING AND REGENERATIVE MEDICINE
J Tissue Eng Regen Med (2015).
Published online in Wiley Online Library (wileyonlinelibrary.com) **DOI:** 10.1002/term.2101

RESEARCH ARTICLE

Partially oxidized polyvinyl alcohol as a promising material for tissue engineering

Elena Stocco[1†], Silvia Barbon[2,5†], Francesca Grandi[3], Pier Giorgio Gamba[3], Luca Borgio[1], Costantino Del Gaudio[4], Daniele Dalzoppo[1], Silvano Lora[2], Senthilkumar Rajendran[1], Andrea Porzionato[5], Veronica Macchi[5], Anna Rambaldo[5], Raffaele De Caro[5], Pier Paolo Parnigotto[1,2] and Claudio Grandi[1]*

[1]*Department of Pharmaceutical and Pharmacological Sciences, University of Padua, Italy*
[2]*Foundation for Biology and Regenerative Medicine, Tissue Engineering and Signalling (TES) ONLUS, Padua, Italy*
[3]*Department of Women's and Children's Health, Paediatric Surgery, University of Padua, Italy*
[4]*Department of Enterprise Engineering 'Mario Lucertini', Intra-Universitary Consortium for Material Science and Technology (INSTM) Research Unit, University of Rome 'Tor Vergata', Italy*
[5]*Section of Human Anatomy, Department of Molecular Medicine, University of Padua, Italy*

Abstract

The desired clinical outcome after implantation of engineered tissue substitutes depends strictly on the development of biodegradable scaffolds. In this study we fabricated 1% and 2% oxidized polyvinyl alcohol (PVA) hydrogels, which were considered for the first time for tissue-engineering applications. The final aim was to promote the protein release capacity and biodegradation rate of the resulting scaffolds in comparison with neat PVA. After physical crosslinking, characterization of specific properties of 1% and 2% oxidized PVA was performed. We demonstrated that mechanical properties, hydrodynamic radius of molecules, thermal characteristics and degree of crystallinity were inversely proportional to the PVA oxidation rate. On the other hand, swelling behaviour and protein release were enhanced, confirming the potential of oxidized PVA as a protein delivery system, besides being highly biodegradable. Twelve weeks after *in vivo* implantation in mice, the modified hydrogels did not elicit severe inflammatory reactions, showing them to be biocompatible and to degrade faster as the degree of oxidation increased. According to our results, oxidized PVA stands out as a novel biomaterial for tissue engineering that can be used to realize scaffolds with customizable mechanical behaviour, protein-loading ability and biodegradability.

Received 16 March 2015; Revised 10 July 2015; Accepted 15 September 2015

Keywords **polyvinyl alcohol; chemical oxidation; biodegradable scaffolds; protein delivery; biomaterials; tissue engineering**

1. Introduction

Biomimetic scaffolds used to control and guide tissue morphogenesis are a new and promising approach in regenerative medicine, which might have great potential in clinical practice (Filová *et al.*, 2013). Considering all biomaterials available to support this strategy, bioactive hydrogels appear to be a primary tool: they can consist of both naturally derived and synthetic polymers (Gnavi *et al.*, 2014). Natural biomaterials are biocompatible but have drawbacks, including poor mechanical strength, relatively high degradation rate, possibility of immune response and often batch-to-batch variability. Synthetic polymers assure a better control over mechanical and chemical properties with no risk of disease transmission; however, they lack bioactivity (Moreira Teixeira *et al.*, 2014). This represents a significant issue, since the local and sustained delivery of paracrine factors may greatly enhance tissue remodelling or organogenesis (Chung and Park, 2007). Amongst synthetic polymers, polyvinyl alcohol (PVA) is widely applied in modern technologies of medicine and pharmacy, due to its biocompatibility, atoxicity and excellent chemical properties. Derived

*Correspondence to: Claudio Grandi, Department of Pharmaceutical and Pharmacological Sciences, University of Padua, Via Marzolo 5, 35131 Padua, Italy. E-mail: claudio.grandi@unipd.it
†These authors contributed equally to this study.

hydrogels and membranes have been extensively developed for both non-implantable and implantable medical materials, as well as for the controlled release of drugs (Pająk *et al.*, 2010; Baker *et al.*, 2012). Similarly, PVA also covers a wide range of applications in different industrial segments, such as textiles, leather, paper and waste water. Its extensive use in industry prompted the research on polymer chemical modifications in order to increase mechanical performance and biodegradation properties (Chiellini *et al.*, 2003). In particular, among post-modifications of PVA, oxidation performed by chemical agents or by microorganisms and enzymes has been an object of interest. The purpose was both to obtain new derivatives (Hassan, 1993; Abdel-Hamid *et al.*, 2001; Malik *et al.*, 2009; Lu *et al.*, 2013) and to enhance polymer biodegradation (Hatanaka *et al.*, 1996; Pająk *et al.*, 2010). Through oxidation, functional groups (i.e. carbonyls) are introduced in the PVA backbone, reducing the formation of intermolecular hydrogen bonds and imparting the polymer different properties, such as lower crystallinity, faster dissolution rate and lower viscosity in aqueous milieux (Lu *et al.*, 2013).

Despite being investigated with highly rewarding outcomes in industry, chemical oxidation has never been reported in the literature to be used in regenerative medicine for the manufacture of tissue substitutes. Based on this evidence, in this study we studied the partial oxidation of PVA to obtain new biosynthetic scaffolds for tissue engineering (TE), which we patented for their innovative end-use destination (Borgio *et al.*, 2013). The aim was to ameliorate the protein/GF release ability and biodegradability properties of hydrogels in comparison with neat PVA.

2. Materials and methods

2.1. Materials and equipment

All the chemicals and reagents were obtained from Sigma-Aldrich (St. Louis, MO, USA) with the following exceptions: potassium permanganate, perchloric acid, sodium hydrogen phosphate, sodium chloride, ethanol, methanol, acetone, ammonium acetate and 2,4-dinitrophenylhydrazine (DNPH) were purchased from Fluka (Basel, Switzerland); phosphate-buffered saline (PBS) tablets were purchased from Gibco Life Technologies (Paisley, UK); hydrochloric acid was obtained from Carlo Erba (Milan, Italy); the dialysis membranes (cut-off 8000 Da) were provided by SpectraPor (Philadelphia, PA, USA); and MilliQ-grade water was prepared with a MilliQ Academic system (Millipore, Bedford, MA, USA).

2.2. Preparation of PVA and oxidized PVA solutions

PVA solution was prepared by suspending in MilliQ water a preweighed quantity of PVA powder [molecular weight (Mw) 146 000–186 000 Da, 99+% hydrolysed]. The powder suspension was then heated for 48 h at 100°C under stirring until the polymer was completely dissolved. Partial oxidation of PVA was obtained using potassium permanganate ($KMnO_4$) in dilute perchloric acid ($HClO_4$). The stoichiometry of the reaction is described by the following equation, referred to a hypothetical vinyl alcohol monomer (–CH_2 CHOH–):

$$2KMnO_4 + 5[CH_2CHOH] + 6HClO_4 \rightarrow 5[CH_2CO] + 2\,Mn(ClO_4)_2 + 8H_2O + 2KClO_4$$

Typically, to prepare 1% oxidized (1% Ox) PVA, 1 g PVA was solubilized in 20 ml MilliQ water and then 5 ml $KMnO_4$ water solution (2.9 mg/ml) and 0.3 ml 70% $HClO_4$ were added; the reaction was run for 1 h at 30°C until a clear solution was obtained. To prepare 2% oxidized (2% Ox) PVA, the amounts of $KMnO_4$ and $HClO_4$ were doubled. After the oxidation step, the resulting solution was dialysed extensively against water using a membrane with 8000 Da cut-off. If not used immediately, oxidized PVA solutions were frozen at –20°C and lyophilized by an under-vacuum evaporator (Speed Vac Concentrator Savant, Instruments Inc., Farmingdale, NJ, USA). In its lyophilized state, partially oxidized PVA is stable at least for 1 year at room temperature (RT). To recover oxidized solutions, lyophilized PVA has to be processed as described above for polymer powder.

2.3. Characterization of oxidized polymer solutions

The contents of carbonyl groups in 1% Ox and 2% Ox PVA were evaluated quantitatively by DNPH assay (Levine *et al.*, 1990) and qualitatively by covalent binding of lysozyme. DNPH assay involves derivatization of the carbonyl group with DNPH, leading to the formation of stable 2,4-dinitrophenyl (DNP) hydrazone products. Briefly, 10 mg lyophilized 1% and 2% oxidized PVA were respectively dissolved at 100°C in 1 ml MilliQ water; 100 µl of these solutions were added to 900 µl 10 mM DNPH in 2.5. M HCl. The PVA-phenylhydrazone derivative reached maximum yield after 48 h at 25°C and was recovered by GPC on a PD-10 column (GE Healthcare, Cleveland, OH, USA). The mobile phase consisted of a mixture of PBS: methanol (70:30 v/v) which was pumped at a flow rate of 1 ml/min. The separation profile was monitored at 375 nm. The first eluted peak corresponded to hydrazones bound to PVA; it was collected and the absorption spectrum was registered using a spectrophotometer Jasco mod V630 (Jasco, Japan). The amount of phenylhydrazone derivatives was evaluated from the absorbance (A) at 375 nm, taking into account a molar absorbtivity (ε) of 22 000 M/cm.

The covalent interaction between oxidized PVA and lysozyme was assessed by the reducing agent sodium cyanoborohydride [$NaBH_3(CN)$]; 20 mg/ml 1% Ox and 2% Ox PVA solutions were incubated with a lysozyme solution in 13 mg/ml PBS at RT in the presence of

DOI: 10.1002/term

2.5mg/ml $NaBH_3(CN)$. At different end-points (4, 24, 50 and 120 h) the solutions were analysed by GPC, using a high-performance column Superose 6 10/300 GL and an HPLC AKTA (GE HealthCare). The absorption profiles of bound and free lysozyme were monitored at 280 nm, with PBS as eluent, at a flow rate of 0.5 ml/min.

The sizes of PVA, 1% Ox and 2% Ox PVA molecules in water were evaluated by Dynamic Light Scattering (DLS). A Zetasizer Nano-ZS DLS instrument (Malvern Instruments Ltd, Worcestershire, UK) was used, under the control of a Peltier unit at 25°C. Solutions containing 3 mg/ml each sample were centrifuged at 15 000 rpm at 22°C for 1 h in a GS-15R centrifuge (Beckman, Brea, CA, USA). A volume of 150 µl of each supernatant was analysed; volume plots were used. The refraction indices considered were those of polystyrene and water for PVA and the dispersing medium, respectively.

2.4. Scaffold preparation

PVA, 1% and 2% oxidized PVA were used to prepare scaffolds by pouring a solution of each between two sheets of plate glass separated by spacers 2 mm thick. Physical crosslinking of polymer solutions occurred through a partially modified freeze–thaw (FT) process, according to Lozinsky *et al.* (1995). Briefly, polymeric aqueous solutions cast into moulds were first frozen at –20°C for 24 h and then thawed at –2.5°C for 24 h.

After three FT cycles, the hydrogels were stored at –20°C until use; under these conditions they are stable at least for 1 year. After thawing, scaffolds can be kept in deionized water at 4°C for 2–3 days.

2.5. Scanning electron microscopy (SEM) analysis

Morphological analysis of scaffolds was performed by SEM. Samples were dehydrated through a series of graded ethanols, exposed to critical-point drying and gold sputtering and finally observed. Images were taken using a JSM-6490 scanning electron microscope (Jeol USA, Peabody, MA, USA).

2.6. Scaffold characterization

The mechanical properties of the hydrogels (5 × 2 × 30 mm; $n = 5$) were evaluated by means of uniaxial tensile tests up to break at 5 mm/min, using a universal testing machine (UTM; Lloyd LRX). All the measurements were recorded after withdrawal of the samples from the storage solution (PBS) under ambient conditions. In order to prevent sliding during the test, the specimens were clamped to the UTM grips by means of two strips of emery paper. Secant modulus at 20% strain, stress and strain at break were calculated.

Thermal characteristics of PVA scaffolds were assessed by means of differential scanning calorimetry (DSC; 200 PC Netzsch-Gerätebau GmbH, Selb, Germany). The samples were first air-dried for 24 h and about 10 mg were then placed in an aluminium pan and heated at a scanning rate of 10°C/min to 250°C. Measurements were carried out in a nitrogen atmosphere. Melting temperature (T_m) and enthalpy (ΔH_m) were evaluated from the first heating scan; the degree of crystallinity was calculated from the melting enthalpy, as follows:

$$X_c = \frac{\Delta H_m}{\Delta H_0} \cdot 100$$

where ΔH_0 is the melting enthalpy of 100% crystalline PVA (138.6 J/g) (Hassan and Peppas, 2000).

Finally, PVA and oxidized PVA hydrogels (5 × 2 × 30 mm) were separately immersed in 5 ml PBS 1× solution at 37°C and 95% relative humidity for a total time of 600 h. Every 24 h, PBS excess was removed by wiping the hydrogels with filter paper and the samples were weighed. The swelling ratio was calculated using the following equation:

$$\text{Swelling}\ (\%) = \frac{W_s - W_d}{W_d} \cdot 100$$

where W_s is the weight of the swollen hydrogel and W_d is the weight of the dry hydrogel.

2.7. Scaffold loading and evaluation of protein release

The protein release ability of PVA, 1% Ox and 2% Ox PVA scaffolds (7 mm diameter × 2 mm thickness) was investigated using BSA (MW 66.5 kDa) and TGFβ1 (MW 25 kDa) as protein models. The scaffolds were soaked in 1 ml BSA solution in 40 mg/ml PBS, pH 7.4, for 24 h at 37°C. Following the incubation period, each scaffold was transferred in 1 ml fresh PBS, which was collected and changed at predetermined end-points (1, 24 and 144 h). The absorption at 280 nm of washing solutions was recorded and the content of BSA was evaluated ($\varepsilon = 0.66$). The resulting data were normalized considering the volumes of the scaffolds. Thereafter, PVA supports were incubated in 1 ml 50 ng/ml TGFβ1 in PBS for 48 h at 37°C. Growth factor release at 24, 48 and 72 h was detected using a FP-6500 fluorimeter (Jasco). The spectra were recorded using a Suprasyl quartz cuvette with excitation and emission optical paths of 10 and 2 mm, respectively. Excitation wavelength was set at 280 nm, while emission spectra were acquired in the range 290–450 nm.

2.8. Evaluation of TGFβ1 release on human primary articular chondrocytes

The effect of TGFβ1 release from PVA and oxidized scaffolds was evaluated on a human primary articular chondrocyte (AC) population. Cells were isolated, cultured and characterized as previously described (Stocco *et al.*, 2014).

DOI: 10.1002/term

A 600 μl suspension of ACs at passage 2 was seeded in a 24-multiwell plate (10 000 cells/cm^2) and a culture plate insert (cut-off 1 μm) was placed inside each well. PVA and oxidized PVA scaffolds were then introduced into the inserts and soaked in 400 μl complete medium. After 72 h and 7 days from seeding, cell proliferation was evaluated by 3-(4,5-dimethylthiazol-2-yl)-2,5-dimethyltetrazolium bromide (MTT) assay. The results were expressed as number of cells grown on the seeded surface.

2.9. *In vivo* study of scaffold biodegradability

All animal procedures were approved by the ethical committee of Padua University, following the guidelines formulated by the Italian Department of Health. The animals were housed in a temperature-controlled facility and were given laboratory rodent diet and water *ad libitum*. Twelve BALB/c mice were gas anaesthetized by isoflurane and oxygen administration; then their dorsal surfaces were shaved and sterile-prepared with Betadine® (Bayer, Leverkusen, Germany) before performing a lombotomic incision of about 20 mm on the right side, using a No. 10 surgical blade (Becton-Dickinson, Franklin Lakes, NJ, USA). A subcutaneous pouch was created using blunt dissection technique and polymer disks (7 mm diameter × 2 mm thickness) of PVA, 1% Ox and 2% Ox PVA (n = 4/group) were inserted in, and anchored to, the latissimus dorsi muscle, using Tycron 4/0 sutures. Following implantation, the skin was stitched using absorbable Novosyn 4/0 sutures. After surgery, the animals were administered anti-inflammatory (Rimadil, 5 mg/kg) and antibiotic (Bytril, 5 mg/kg) therapy for 5 days and were allowed to recover in the cage. Twelve weeks after implantation, the mice were euthanized by carbon dioxide asphyxiation. The implants and surrounding tissues were excised and the scaffolds were preliminarily analysed for their size and integrity compared to unimplanted controls. Samples were also fixed with 2.5% glutaraldehyde in 0.1 M cacodylate buffer, pH 7.2, for SEM investigation. Samples for histological and immunohistochemical analysis were frozen and embedded in OCT or fixed in 10% formalin solution in neutral PBS and embedded in paraffin.

2.10. Histological and immunohistochemical analysis

Samples embedded in OCT were cut into 10 μm-thick serial sections and stained with haematoxylin and eosin (H&E). They were mainly used for the evaluation of PVA characteristics and state of degradation. Paraffin-embedded samples were cut into 5 μm-thick serial sections; the sections were then dewaxed and rehydrated according to routine protocols. Immunological characterization of the cells identified in contiguity with PVA was carried out with the following antibodies diluted in PBS: anti-CD3 (polyclonal rabbit anti-human CD3, A 0452; Dako, Milan, Italy) diluted 1:500; anti-F4/80 (sc-26643-R; Santa Cruz Biotechnology, CA, USA) diluted 1:800. Sections were incubated in 1% hydrogen peroxide in deionized H_2O to remove endogenous peroxidase activity and enhance antibody penetration into the tissue, and then washed in 0.01 M PBS. For both protocols, antigen unmasking was performed with 10 mM sodium citrate buffer, pH 6.0, at 90°C for 10 min. The sections were then incubated for 30 min in blocking serum [0.04% bovine serum albumin (BSA; A2153, Sigma-Aldrich, Milan, Italy) and 0.5% normal goat serum (X0907, Dako, Carpinteria, CA, USA) to eliminate unspecific binding, and then incubated for 1 h at room temperature with the above primary antibodies. Primary antibody binding was revealed by incubation with anti-rabbit/mouse serum diluted 1:100 in blocking serum for 30 min at room temperature (Dako® EnVision + TM peroxidase, rabbit/mouse; Dako, Glostrup, Denmark) and developed in 3,3′-diaminobenzidine for 3 min at RT. Lastly, the sections were counterstained with haematoxylin. As a negative control, sections were incubated without primary antibodies.

2.11. Statistics

Results are expressed as mean ± standard deviation (SD). The data were processed using SPSS v. 19.0 software (SPSS Inc., USA). Statistical analysis to assess differences between groups was performed in two steps: first, data were compared using the Kruskal–Wallis non-parametric test; if significant differences were found, groups were compared individually using the Mann–Whitney U-test; $p < 0.05$ was considered significant.

3. Results and discussion

3.1. Characterization of oxidized polymers

Biomaterials play an important role in most tissue-engineering strategies (Shin *et al.*, 2003): their selection constitutes a key point for the success of tissue defect treatments following disease or trauma (Armentano *et al.*, 2010). Hydrogels are promising biomaterials for tissue regeneration, being widely investigated for their potential use in soft tissue engineering (Gkioni *et al.*, 2010) as space-filling agents, vehicles for bioactive molecules and three-dimensional (3D) structures for cell proliferation and specific induction (Drury and Mooney, 2003). Among synthetic polymers, PVA hydrogels stand out: Food and Drug Administration (FDA) and Conformité Européenne (CE) have already approved them for clinical use in humans, due to their excellent biocompatibility and safety (Ino *et al.*, 2013). Despite having an extensive history of biomedical applications, neat PVA suffers from significant shortcomings: physical crosslinking leads to stronger polymer–polymer chain interactions, loss of biodegradation rate and less controlled drug release (Fejerskov *et al.*, 2013); hence, re-engineering of PVA to

DOI: 10.1002/term

improve degradation and control drug release appears highly rewarding. Because of that, the present study reports the development and the characterization of chemically oxidized PVA for the manufacture of novel biodegradable crosslinked scaffolds, able to vehicle proteins and promote tissue regeneration. To our knowledge, this is the first study that considers partial oxidation of PVA to prepare scaffolds for tissue engineering. In particular, in the perspective of *in vivo* implant, the 1% and 2% degrees of oxidation were retained to be the most adequate. In fact, in the case of *in vivo* cleavage at oxidation sites, the fragments produced will be, on average, no longer than 100 monomers and no heavier than 4400 Da, being easily excreted at the renal level (Holechek, 2003). Moreover, we assessed that a degree of oxidation $>$ 2% is not eligible to obtain scaffolds, as the polymer solutions no longer crosslink.

After the oxidation process, PVA carbonyl content was determined by DNPH assay. 2,4-Dinitrophenylhydrazine is typically used to determine carbonyl groups of aldehydes and ketones; reacting with carbonyls, it leads to the formation of hydrazone derivatives (Figure 1A). GPC chromatograms of PVA carbonyls after reaction with DNPH are reported in Figure 1B; as shown, with increasing degree of oxidation a higher amount of hydrazone was detected. Average carbonyl content was equal to 5 μM/mg and 11.4 μM/mg in 1% Ox and 2% Ox PVA, respectively. PVA was considered as a negative control.

Sodium cyanoborohydride is a reducing agent that was used to establish a stable covalent interaction between carbonyl groups of oxidized PVA and amino groups of lysozyme, through reduction of intermediate Schiff's bases, otherwise not stable. By GPC, we obtained chromatograms of 1% Ox (Figure 1C) and 2% Ox (Figure 1D) PVA incubated with lysozyme at different end-points (4, 24, 50 and 120 h). After 4 h of incubation, the typical band absorbing at 280 nm is recognizable. After 24 h, the lysozyme bound to polymers reached about 22% (1% Ox PVA) and 45%

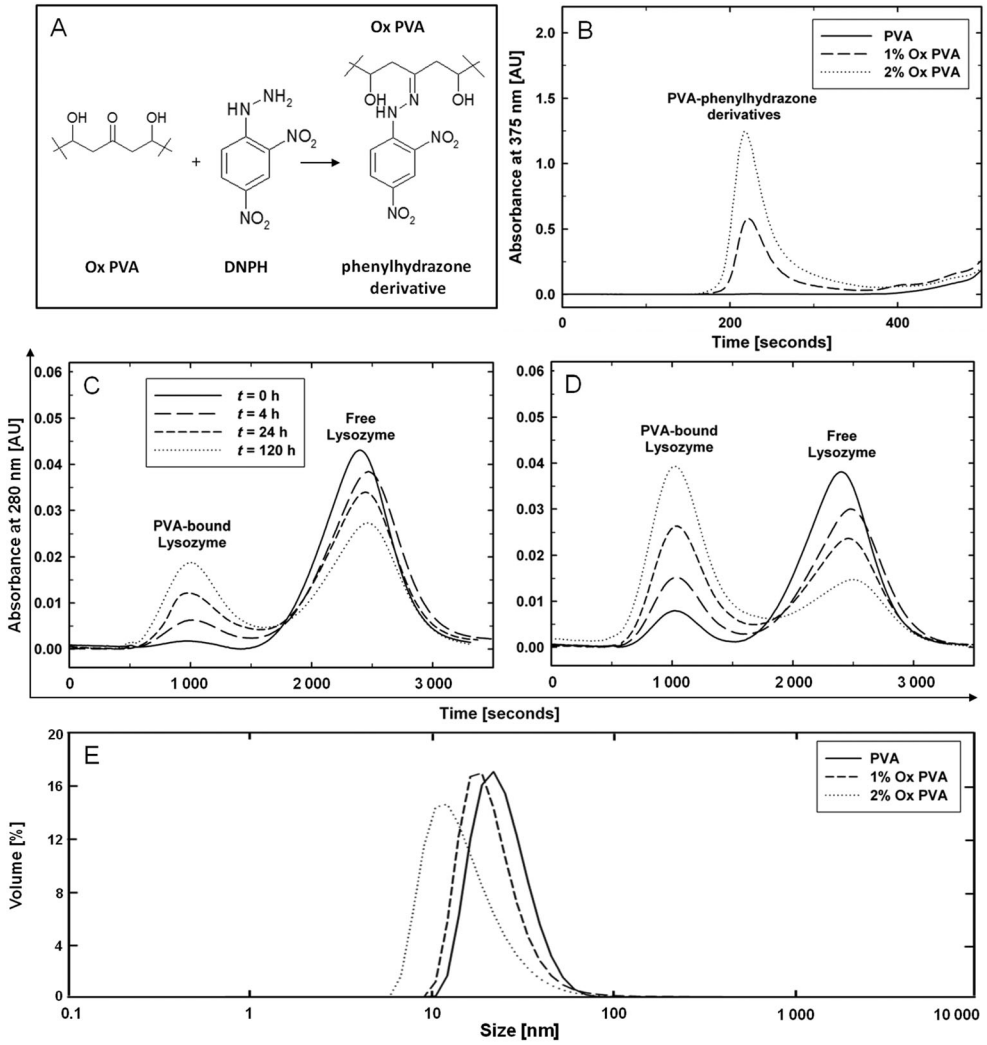

Figure 1. Investigation of oxidized PVA. (A) Chemical reaction between oxidized PVA and DNPH. (B) GPC profiles of PVA, 1% and 2% Ox PVA after DNPH treatment: peaks represent size exclusion chromatograms of high molecular weight phenylhydrazone derivatives, which increase along with degree of oxidation of PVA; free DNPH profile is not shown. (C, D) GPC evaluation of covalent interaction between lysozyme and 1% (C) and 2% Ox (D) PVA: due to the introduction of functional carbonyl groups, 1% and 2% Ox PVA bound higher amounts of lysozyme than neat PVA. (E) DLS analysis of PVA and oxidized PVA molecules, typical measurement of particle size distribution in percentage volume: along with degree of oxidation, the hydrodynamic radii of the particles decreased; note the broader distribution peak of 2% Ox PVA, ascribable to higher polydispersity

DOI: 10.1002/term

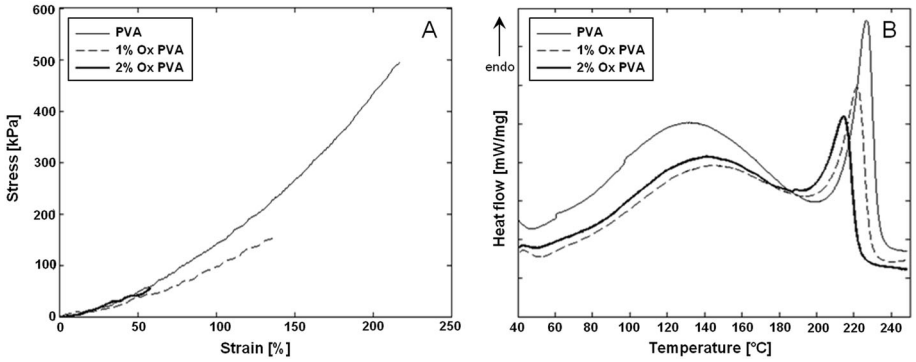

Figure 2. Mechanical and physical properties. (A) Stress–strain curves of uniaxial tensile tests performed on PVA and oxidized PVA; polymer stiffness decreased as degree of oxidation increased. (B) DSC thermograms of PVA and oxidized PVA samples; oxidation treatment can influence polymer thermal properties

(2% Ox PVA) of the initial total amount. Bound lyzozyme increased progressively up to 120 h. Beyond chemical characterization, covalent interaction with lysozyme allowed us to predict the ability of oxidized PVA to form covalent binding, even with RGD sequences or oligopeptides, which is useful to functionalize scaffold surface.

The long, string-like nature of the polymer backbones causes them to take on a variety of complex, coiled conformations which can greatly affect the macroscopic properties of the derived scaffold. Hence, the size and size distribution of polymer chains of neat and oxidized PVA in water were investigated by DLS. Figure 1E reports polymer particles size distribution by volume. The mean hydrodynamic radius was about 28 nm for PVA, 23 nm for 1% Ox PVA and 16 nm for 2% Ox PVA. The shift between the maximum of the three curves represents a decrease of the mean size of the particles; the areas below the curves show the extent of dimensional dispersion. As highlighted by our data, the oxidation process determines reduction in the hydrodynamic radius and higher polydispersity of the particles.

As polymers in good solvents are shaped like expanded coils, the hydrodynamic radius calculated by DLS corresponds to the apparent size of the dissolved particle. The hydrodynamic radius is directly proportional to the end-to-end distance that characterizes the average spatial dimensions of the coils. Considering that, the decrease of hydrodynamic radius along with degree of oxidation confirms the shortening of the polymer chains due to chemical modification.

3.2. Scaffold characterization

In tissue engineering, biomaterial selection and scaffold design play a vital role in the expected outcome. The choice of polymer is crucial in this regard, as it should be specifically tailored for the target tissue to be regenerated or the therapeutic function to be achieved. Physical parameters (such as crosslinking density, mechanical strength and crystallinity) can surely affect polymer behaviour in mimicking biological tissues. Our study demonstrated that PVA hydrogels prepared via a freeze–thaw method can be chemically modified in order to adjust their characteristics, depending on specific tissue-engineering applications.

As far as mechanical behaviour is concerned, PVA hydrogels were analysed by uniaxial tensile tests. Representative stress–strain curves of samples are reported in Figure 2A, while mechanical properties are summarized in Table 1. The mechanical response was clearly affected by the oxidation treatment, highlighting that PVA possesses better strength and stiffness than its chemically oxidized counterparts, with the help of available hydroxyl groups involved in intra- and intermolecular hydrogen bonding (Gupta *et al.*, 2011). Thus, hydrogel mechanics can be modified by altering the number of crosslinkable groups/chain. It is then reasonable to plan a tissue-engineering regenerative strategy based on the modulation of the mechanical response of PVA for the replacement of more or less resistant soft tissues, such as cartilage, tendon, gut, nerves and vessels. In parallel, the DSC analysis was carried out. Thermograms are shown in Figure 2B, while the results are summarized in Table 2. Samples were characterized by an endothermic broad band in the range 80–160°C, which can be ascribed to the evaporation of residual water. The melting of PVA is represented by a sharp peak, whose intensity decreases as oxidation rate increases (Figure 2B). Oxidation seems to affect both PVA melting temperature and degree of crystallinity, which lower as carbonyl content rises (Table 2).

The hydrogen bonding between hydroxyl groups of PVA and water also governs the crystallinity of the bulk PVA material (Nagura *et al.*, 1989): DSC analysis highlighted that oxidation treatment can influence even polymer

Table 1. Mechanical properties of PVA gels

	Secant modulus (kPa)	Stress at break (kPa)	Strain at break (%)
PVA	52.0 ± 13.4	330.0 ± 116.6	192 ± 23
1% Ox PVA	42.9 ±16.5	152.8 ± 25.8$^{\#}$	162 ± 18
2% Ox PVA	21.5 ± 9.2$^{\#}$	68.0 ± 18.3$^{\#}$*	78 ± 15$^{\#}$*

Following chemical oxidation, mechanical properties of PVA were modulated, as shown by secant modulus, stress at break and strain at break progressive reduction for 1% and 2% Ox PVA.
$^{\#}p < 0.05$ with respect to PVA.
*$p < 0.05$ with respect to 1% Ox PVA).

DOI: 10.1002/term

Table 2. Thermal properties of PVA gels

	T_m (°C)	ΔH_m (J/g)	X_c (%)
PVA	226.8	43.1	31.1
1% Ox PVA	221.8	34.0	24.5
2% Ox PVA	214.6	25.0	18.0

Hydrogel T_m and ΔH_m decreased slightly along with degree of oxidation, indicating a gradual loss of crystallinity, as shown by X_c calculated values.

thermal properties, such as melting temperature, enthalpy and crystallinity. In particular, neat PVA was found to be more crystalline than its oxidized counterparts and, as such, it is expected to withstand degradation for a longer period, since the crystalline regions are more resistant to hydrolytic attack than the amorphous regions (Santos *et al.*, 1999). This means that thermal property study allowed us to predict a higher biodegradation rate for 1% and 2% Ox PVA in view of the *in vivo* implant.

3.3. Swelling behaviour and protein release capacity

In addition to their promising biocompatibility characteristics, PVA hydrogels are particularly desirable in the biomedical field, due to their sensitivity in the physiological or biological environment where they are used. In recent years, much research has focused on the development and analysis of environmentally responsive hydrogels exhibiting swelling changes due to modification of intrinsic properties or external conditions (Peppas *et al.*, 2000). When a biopolymer network is in contact with an aqueous solution or a biological fluid, the network starts to swell due to the thermodynamic compatibility of the polymer chains and water. The swelling force is counterbalanced by the retractive force induced by the crosslinks of the network. Swelling equilibrium is reached when these two forces are equal.

The behaviour of PVA scaffolds after 288 h of incubation in PBS solution is shown in Figure 3A. Both 1% and 2% Ox PVA hydrogels showed a rapid swelling ratio of 60% and 110%, respectively, within 24 h. Subsequently, the swelling ratios decelerated until an equilibrium was reached at approximately 70% (1% Ox PVA) and 40% (2% Ox PVA) mass increase after about 288 h, then remaining stable over the course of the experiment. Conversely, PVA hydrogels displayed different swelling ratios, increasing in mass by about 20% within 24 h; swelling continued, albeit at a slower rate, until equilibrium was reached after approximately 288 h. Given the swelling capacity, BSA release was investigated at different end-points to assess the potential of scaffolds for controlled drug delivery. In Figure 3B, results are shown as μg released BSA/ml hydrogel. Oxidized scaffolds sustained protein delivery better than PVA; in particular,

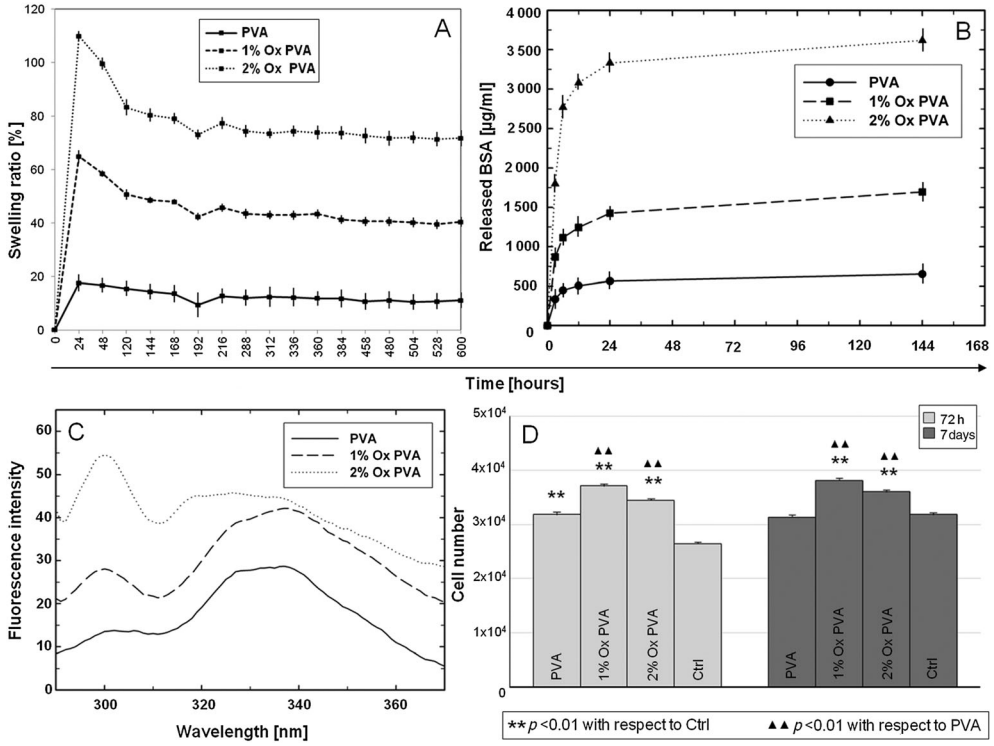

Figure 3. Swelling behaviour and protein release. (A) Swelling ratio as a function of time for crosslinked PVA, 1% and 2% Ox PVA hydrogels in PBS at 37°C: by 24 h, all samples showed the maximum swelling ratio; equilibrium was reached after about 288 h in solution. (B) BSA release profiles of PVA and oxidized PVA scaffolds; protein release was higher for 2% Ox PVA and 1% Ox PVA than for neat PVA. (C) Emission spectra of washing solutions after incubation of PVA and oxidized PVA hydrogels with TGFβ1; the peak at nearly 300 nm is due to tyrosine, while the broad band on the right is ascribable to tryptophan. (D) Chondrocyte proliferation after 72 h and 7 days of co-culture with TGFβ1-loaded PVA, 1% and 2% Ox PVA scaffolds; cell growth rate seemed to be stimulated by the higher amount of TGFβ1 released by oxidized PVA

DOI: 10.1002/term

an initial exponential release was clear within 24 h; afterwards, according to UV spectra, protein release was sustained up to 144 h. Moreover, BSA release data allowed us to learn about the protein-loading capacity of the scaffolds: the amount of BSA released at 144 h can be considered as the maximum adsorbed by the hydrogels, since the release kinetic reached a plateau phase. Given that, the relative loading capacity of 1% Ox PVA and 2% Ox PVA scaffolds was respectively 2.6 and 5.6 times higher than the adsorption capacity of neat PVA. As for release ability, loading capacity was shown to increase linearly along with the degree of oxidation.

In parallel, TGFβ1 release was evaluated by measuring the fluorescence intensity of GF-loaded scaffold washing solutions; after 72 h of incubation, the fractions were pooled and their fluorescence was measured. Figure 3C reports the emission spectra of the washing solutions: the peak at nearly 300 nm was due to tyrosine, while the broad band on the right is ascribable to tryptophan. Fluorometric analysis highlighted that released TGFβ1 increased along with scaffold oxidation rate. As TGFβ1 shows a promising potential in promoting chondrocyte proliferation (Leipzig *et al.*, 2006), a MTT assay was performed on articular chondrocytes co-cultured with loaded

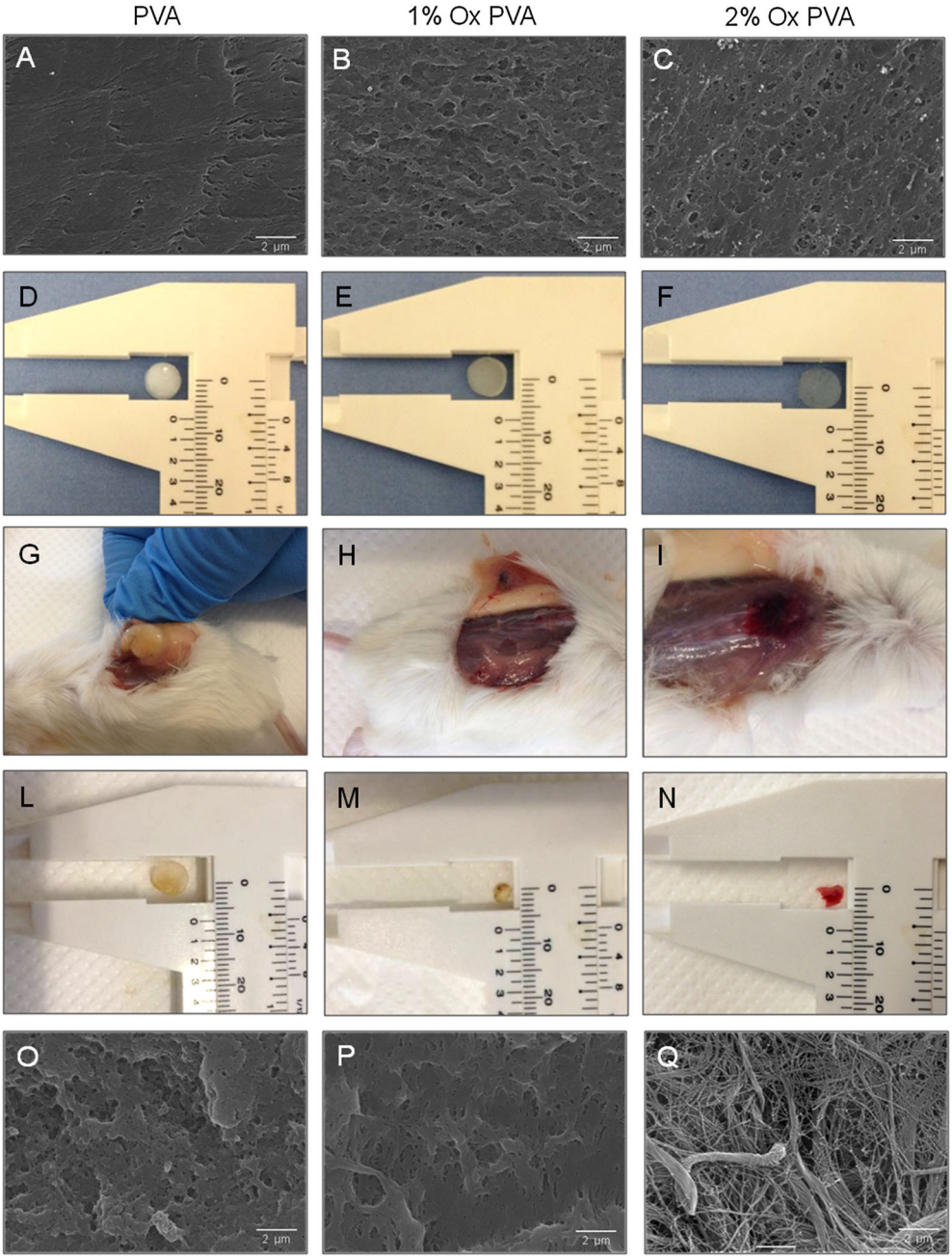

Figure 4. ***In vivo*** **biodegradation. (A–C, O–Q) SEM investigation of PVA and oxidized PVA scaffold surface morphology: pre-implant micrographs (A–C) show that structural remodelling occurs with increasing degree of oxidation; after 12 weeks of** ***in vivo*** **implantation, explanted PVA (O) and 1% Ox PVA (P) scaffolds showed typical polymeric surface features; otherwise, 2% Ox PVA explant (Q) was replaced by collagen fibres. (D–N) Gross appearance of pre-implant (D, E, F) and explanted (L, M, N) PVA, and oxidized PVA scaffolds; in (G–I) implants are shown before removal (12 weeks after surgery)**

DOI: 10.1002/term

scaffolds. A significant increase of proliferative activity assessed effective TGFβ1 loading and release; 72 h after seeding, cells co-cultured with 1% Ox and 2% Ox PVA showed a higher proliferation rate ($p < 0.01$) compared to chondrocyte–PVA co-cultures. The same trend was also recorded at 7 days after seeding (Figure 3D). These results, beyond highlighting the effectiveness of oxidized PVA in loading and releasing proteins, allowed us to rule out any cytotoxic activity exerted by the hydrogels.

As demonstrated, the introduction of carbonyls on the PVA backbone supported the protein-loading ability of the scaffolds. This should be ascribable to a possible Schiff-base interaction between the amino groups of proteins and carbonyls of oxidized PVA and/or to the higher swelling ratio. Our results confirmed that integrating controlled release strategies within hydrogels may lead to a novel delivery platform able to control and guide tissue regeneration.

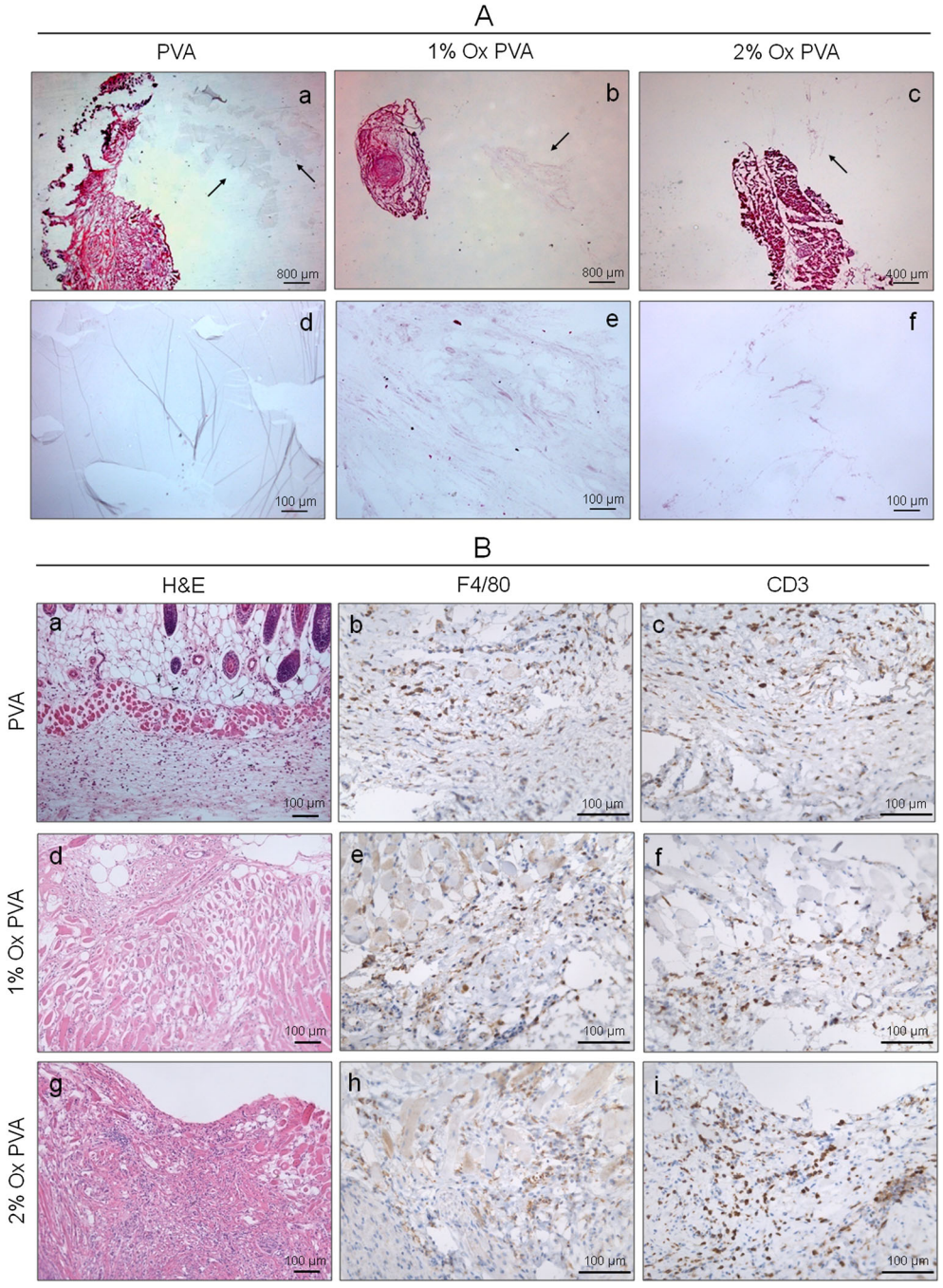

Figure 5. Investigation of PVA explants. (A) Histological analysis by (H&E) staining of PVA scaffolds explanted after 12 weeks of *in vivo* subcutaneous implantation: note the absence of degradation and cell infiltration of PVA scaffold, ruptures and folding being ascribable to post-sampling artefactual changes (a, d); conversely, 1% (b, e) and 2% (c, f) Ox PVA appeared much more compromised after exposure to biological fluids, being the second one almost no longer visible next to the implant site. (B) Evaluation of inflammatory cell infiltration: (a, d, g) H&E staining of biological tissues surrounding scaffolds after 3 months of *in vivo* subcutaneous implantation; (b, c, e, f, h, i) immunohistochemical investigation for localization of F4/80$^+$ and CD3$^+$ cells on samples; note more numerous lymphomonocytic cells after implant of 2% oxidized PVA

DOI: 10.1002/term

3.4. *In vivo* scaffold degradation

As already highlighted above, we considered chemical modification to promote the biodegradation of crosslinked PVA; oxidation treatment is an important step in biodegradation (Hatanaka *et al.*, 1996). Most biodegradable polymers suffer from a short half-life, due to rapid degradation upon implantation, high stiffness and limited ability to functionalize their surface with chemical moieties (Wang *et al.*, 2010). Combining material chemistry and processing technology, it is possible to tune the scaffold degradation rate. The aim is to match the tissue growth rate so that the regenerated tissue may progressively replace the scaffold.

Before *in vivo* implantation, SEM micrographs were obtained to characterize the superficial morphology of the scaffolds, investigating contingent differences related to oxidation. According to this analysis, PVA scaffolds showed a smooth and regular surface (Figure 4A). Conversely, 1% and 2% oxidized PVA supports had a different morphology, characterized by a rough surface (Figure 4B, C).

After the surgical procedures, no implanted mice were euthanized or died prematurely due to scaffold-related complications. Careful surveillance of the mice in the weeks after surgery showed neither systemic signs of infection nor local signs of rejection or inflammation.

At the end of the 12-week period after *in vivo* implantation, preliminary evidence was gathered. The size and integrity of explanted oxidized scaffolds were visually compromised (Figure 4M, N) compared to pre-implant supports (Figure 4E, F). In particular, the degradation rate increased along with the degree of oxidation of PVA. Conversely, PVA scaffolds did not show remarkable biodegradation: the gross appearance after explantation was similar to the pre-implant one (Figure 4D, L). To our knowledge, this is the first time that the oxidized PVA biodegradation profile has been studied *in vivo*.

SEM analysis was repeated on scaffolds after explantation and highlighted surface differences between PVA, 1% Ox and 2% Ox PVA scaffolds (Figure 4O–Q). In particular, both PVA and 1% Ox PVA explants showed an identifiable polymeric structure (Figure 4O, P), even though their surface appeared deteriorated in comparison to pre-implant controls (Figure 4A, B). Conversely, the 2% Ox PVA surface was no longer recognizable: SEM images revealed the presence of disorganized collagen fibres (Figure 4Q), which should be attributed to scaffold reabsorption and substitution by new connective components.

3.5. Histological and immunohistochemical analysis

OCT-embedded samples proved more useful for the evaluation of PVA characteristics, as PVA underwent volume changes and modifications of its characteristics along the various processing phases of formalin-fixed samples. Also, in frozen samples, PVA sections were very difficult to obtain without ruptures, dislocations or folds (Figure 5A). Apart from artefactual modifications observed during explant sectioning and reported in the literature (Allen *et al.*, 2004), neat PVA texture was intact (Figure 5Ad), without areas of degradation and reabsorption. Conversely, 1% Ox PVA showed partial degradation (Figure 5Ae) and 2% Ox PVA was nearly invisible (Figure 5Af) because of significant degradation, in spite of exhaustive serial sectioning of the samples. No cellular adhesion could be detected over the surface of the biomaterials. Furthermore, while the PVA–hydrogel surfaces remained smooth and transparent, oxidized PVA sections were amorphous and opaque (Figure 5A).

Paraffin-embedded samples were mainly used for specific analysis of the tissues surrounding the implanted materials (Figure 5B). In all the samples, in both PVA and oxidized PVAs, severe inflammatory reactions were not present apart from a slight infiltration of the connective tissue that surrounds the implanted material. In particular, 2% Ox PVA implants seemed to cause a slightly higher infiltration of the surrounding connective tissues. In case of immunological characterization, most infiltrating cells were positive for CD3 or F4/80, suggesting a possible role for lymphomonocytic cells in implant reabsorption. In fact, 2% Ox PVA was nearly invisible as a hydrogel disc, indicating considerable replacement by new connective components, as confirmed by the SEM results. In parallel, sections incubated without primary antibodies showed no immunoreactivity, confirming the specificity of the immunostaining.

5. Conclusions

The current research led to the development and characterization of novel PVA-derived scaffolds obtained by partial polymer oxidation. Oxidized PVA polymers showed customizable mechanical behaviour, protein-loading ability, biocompatibility and biodegradability *in vivo*, making them suitable for prospective *in situ* tissue-engineering applications. Future investigations will also focus on the employment of oxidized PVA scaffolds for the development of tissue substitutes. Our aim was to show that oxidized PVA can meet the requirements of a wide range of tissues by virtue of their versatility. Such hydrogels could contribute to biomaterial science for tissue-engineering applications, covering the lack of tailorable biomaterials able to closely match the physiological properties of natural tissues.

Conflict of interest

The authors have declared that there is no conflict of interest.

Acknowledgements

This study was supported by Padua University and Fondazione TES Onlus (Padua).

Author contributions

E.S. and S.B. designed and performed research, analysed and interpreted data and wrote the manuscript; F.G. and P.G.G. performed and supervised *in vivo* experiments; C. D.G. performed and supervised mechanical and physical characterization of hydrogels and analysed and interpreted data; L.B., D.D., S.L. and S.R. performed research and analysed and interpreted data; A.P., V.M. and A.R. performed histological and immunohistochemical analysis and interpreted data; R.D.C., P.P.P. and C.G. conceived and designed experiments, supervised data analysis and interpretation and made the final approval of the manuscript; all authors read and approved the final manuscript.

References

Abdel-Hamid MI, Ahmed GAW, Hassan RM. 2001; Kinetics and mechanism of oxidation of poly(vinyl alcohol) macromolecule by chromic acid in aqueous perchloric acid. *Eur Polym J* **37**: 2201–2206.

Allen MJ, Schoonmaker JE, Bauer TW *et al.* 2004; Preclinical evaluation of a poly(vinyl alcohol) hydrogel implant as a replacement for the nucleus pulposus. *Spine (Phila PA 1976)* **29**: 515–523.

Armentano I, Dottori M, Fortunati E *et al.* 2010; Biodegradable polymer matrix nanocomposites for tissue engineering: a review. *Polym Degrad Stabil* **95**: 2126–2146.

Baker MI, Walsh SP, Schwartz Z *et al.* 2012; A review of polyvinyl alcohol and its uses in cartilage and orthopedic applications. *J Biomed Mater Res B Appl Biomater* **100**: 1451–1457.

Borgio L, Grandi C, Dalzoppo D. 2013; Biomateriale per dispositivi medici, in particolare protesi. Patent No. VI2013A000019, Class A61K. Deposited in 'Camera di Commercio Industria, Artigianato e Agricoltura' of Vicenza, Italy

Chiellini E, Corti A, D'Antone S *et al.* 2003; Biodegradation of poly(vinyl alcohol) based materials. *Prog Polym Sci* **28**: 963–1014.

Chung HJ, Park TG. 2007; Surface engineered and drug releasing prefabricated scaffolds for tissue engineering. *Adv Drug Deliv Rev* **59**: 249–262.

Drury JL, Mooney DJ. 2003; Hydrogels for tissue engineering: scaffold design variables and applications. *Biomaterials* **24**: 4337–4351.

Fejerskov B, Smith AA, Jensen BE *et al.* 2013; Bioresorbable surface-adhered enzymatic microreactors based on physical hydrogels of poly(vinyl alcohol). *Langmuir* **29**: 344–354.

Filová E, Rampichová M, Litvinec A *et al.* 2013; A cell-free nanofiber composite scaffold regenerated osteochondral defects in miniature pigs. *Int J Pharm* **447**: 139–149.

Gkioni K, Leeuwenburgh SC, Douglas TE *et al.* 2010; Mineralization of hydrogels for bone regeneration. *Tissue Eng B Rev* **16**: 577–585.

Gnavi S, Di Blasio L, Tonda-Turo C *et al.* 2014; Gelatin-based hydrogel for vascular endothelial growth factor release in peripheral nerve tissue engineering. *J Tissue Eng Regen Med* DOI: 10.1002/term.1936. [Epub ahead of print]

Gupta S, Webster TJ, Sinha A. 2011; Evolution of PVA gels prepared without crosslinking agents as a cell adhesive surface. *J Mater Sci Mater Med* **22**: 1763–1772.

Hassan CM, Peppas NA. 2000; Structure and morphology of freeze/thawed PVA hydrogels. *Macromolecules* **33**: 2472–2479.

Hassan RM. 1993; New coordination polymers. III: Oxidation of poly(vinyl alcohol) by permanganate ion in alkaline solutions. Kinetics and mechanism of formation of intermediate complex with a spectrophotometric detection of manganate(vi) transient species. *Polym Int* **1**: 5–9.

Hatanaka T, Hashimoto T, Kawahara T *et al.* 1996; Biodegradability of oxidized poly(vinyl alcohol). *Biosci Biotechnol Biochem* **60**: 1861–1863.

Holechek MJ. 2003; Glomerular filtration: an overview. *Nephrol Nurs J* **30**: 285–290.

Ino JM, Chevallier P, Letourneur D *et al.* 2013; Plasma functionalization of poly(vinyl alcohol) hydrogel for cell adhesion enhancement. *Biomater* **3**e25414: 1–7.

Leipzig ND, Eleswarapu SV, Athanasiou KA. 2006; The effects of TGF-β1 and IGF-I on the biomechanics and cytoskeleton of single chondrocytes. *Osteoarthr Cartilage* **14**: 1227–1236.

Levine RL, Garland D, Oliver CN *et al.* 1990; Determination of carbonyl content in oxidatively modified proteins. *Methods Enzymol* **186**: 464–478.

Lozinsky VI, Solodova EV, Zubov AL *et al.* 1995; Study of cryostructuration of polymer systems. XI. The formation of PVA cryogels by freezing–thawing the polymer aqueous solutions containing additives of some polyols. *J Appl Polym Sci* **58**: 171–177.

Lu Y, Kong QM, Jing R *et al.* 2013; Solid state oxidation of polyvinyl alcohol by hydrogen peroxide-Cu(II). *Polym Degrad Stab* **98**: 1103–1109.

Malik MA, Mohammad Ilyas M, Khan Z. 2009; Kinetics of permanganate oxidation of synthetic macromolecule poly(vinyl alcohol). *Ind J Chem* **48**: 189–193.

Moreira Teixeira LS, Patterson J, Luyten FP. 2014; Skeletal tissue regeneration: where can hydrogels play a role? *Int Orthop* **38**: 1861–1876.

Nagura M, Hamano T, Ishikawa H. 1989; Structure of poly(vinyl alcohol) hydrogel prepared by repeated freezing and melting. *Polymer* **30**: 762–765.

Pająk J, Ziemski M, Nowak B. 2010; Poly(vinyl alcohol) – biodegradable vinyl material. *Chemik* **64**: 523–530.

Peppas NA, Huang Y, Torres-Lugo M *et al.* 2000; Physicochemical foundations and structural design of hydrogels in medicine and biology. *Annu Rev Biomed Eng* **2**: 9–29.

Santos CA, Freedman BD, Leach KJ *et al.* 1999; Poly(fumaric-co-sebacic anhydride). A degradation study as evaluated by FTIR, DSC, GPC and X-ray diffraction. *J Control Release* **60**: 11–22.

Shin H, Jo S, Mikos AG. 2003; Biomimetic materials for tissue engineering. *Biomaterials* **24**: 4353–4364.

Stocco E, Barbon S, Dalzoppo D *et al.* 2014; Tailored PVA/ECM scaffolds for cartilage regeneration. *Biomed Res Int* **2014**: 762189.

Wang J, Bettinger CJ, Langer RS *et al.* 2010; Biodegradable microfluidic scaffolds for tissue engineering from amino alcohol-based poly(ester amide) elastomers. *Organogenesis* **6**: 212–216.